Primordial magnetic fields and CMB anisotropies

KANDASWAMY SUBRAMANIAN

IUCAA, Post Bag 4, Pune University Campus, Ganeshkhind, Pune 411 007, India

Abstract. Possible signatures of primordial magnetic fields on the Cosmic Microwave Background (CMB) temperature and polarization anisotropies are reviewed. The signals that could be searched for include excess temperature anisotropies particularly at small angular scales below the Silk damping scale, B-mode polarization, and non-Gaussian statistics. A field at a few nG level produces temperature anisotropies at the 5μK level, and B-mode polarization anisotropies 10 times smaller, and is therefore potentially detectable via the CMB anisotropies. An even smaller field, with $B_0 < 0.1$ nG, could lead to structure formation at high redshift $z > 15$, and hence naturally explain an early re-ionization of the Universe.

Key words: cosmic microwave background – cosmology: theory – magnetic fields

1. Introduction

Magnetic fields are ubiquitous in astrophysical systems but their origin is still a mystery. One possibility is that they arise due to the dynamo amplification of small seed fields. The dynamo paradigm has been extensively studied (cf. Brandenburg & Subramanian 2005 for a recent review), but potential problems remain to be surmounted. These involve the question of whether mean field dynamo coefficients for the galactic dynamo are catastrophically quenched or not, and whether fields generated by the fluctuation dynamo in clusters have a sufficient degree of coherence to explain the observations (Subramanian, Shukurov & Haugen 2006; Shukurov, Subramanian & Haugen 2006; Schekochihin et al. 2005).

An interesting alternative is that the observed large-scale magnetic fields are a relic from the early Universe, arising perhaps during inflation or some other phase transition (Turner & Widrow 1988; Ratra 1992; and reviews by Widrow 2002; Giovannini 2005a). It is well known that scalar (density or potential) perturbations and gravitational waves (or tensor perturbations) can be generated during inflation. Could magnetic field perturbations could also be generated? Indeed mechanisms involving, say, string theory, for the generation of primordial fields have been reviewed in this meeting (Gasperini 2006 and references therein). These generically involve the breaking of the conformal invariance of the electromagnetic action, and the predicted amplitudes are rather model dependent. Nevertheless, if a primordial magnetic field with a present-day strength of $B \sim 10^{-9}$ G and coherent on Mpc scales is generated, it can strongly influence Galaxy formation. An even weaker field, sheared and amplified due to flux freezing, during galaxy and cluster formation may ease the problems of the dynamo. It is then worth considering if one can detect or constrain such primordial fields.

Here we review possible probes of primordial magnetic fields, which use CMB temperature and polarization anisotropies. Indeed there are also a number of puzzling features associated with current CMB observations, which are not fully understood. These include (a) the excess power in temperature anisotropies detected by the Cosmic Background Imager (CBI) experiment on small angular scales (Readhead et al. 2004), (b) the observations by the Wilkinson Microwave Anisotropy Probe (WMAP) satellite for an unexpectedly high redshift of re-ionization (Kogut et al. 2003), (c) the low CMB quadrupole anisotropy seen compared to theoretical expectations (cf. Spergel et al. 2003), and (d) various asymmetry and alignment effects (cf. de Oliveira-Costa et al. 2004). Such features also encourage us to keep open possibilities of new physical effects, perhaps having to do with primordial fields!

2. Magnetic field evolution in the early Universe

Primordial magnetogenesis scenarios generally lead to fields which are Gaussian random, characterized by a spectrum $M(k)$ (see below). This spectrum is normalized by giving the field strength B_0, at some fiducial scale and as measured at the present epoch, assuming it decreases with expansion as $B = B_0/a^2(t)$, where $a(t)$ is the expansion factor. We take B_0 to be a free parameter since the predictions for its value from magnetogenesis theories are highly model and parameter sensitive. Note that the magnetic and radiation energy

densities both scale with expansion as $1/a^4$. So we can characterize the magnetic field effect by the ratio $B_0^2/(8\pi\rho_{\gamma 0}) \sim 10^{-7}B_{-9}^2$ where $\rho_{\gamma 0}$ is the present-day energy density in radiation, and $B_{-9} = B_0/(10^{-9}G)$. Magnetic stresses are therefore small compared to the radiation pressure for nG fields. The scalar, vector and tensor parts of the perturbed stress tensor associated with magnetic fields lead to corresponding metric perturbations. Further the compressible part of the Lorentz force leads to compressible (scalar) fluid velocity and associated density perturbations, while its vortical part leads to vortical (vector) fluid velocity perturbation. The magnetically induced compressible fluid perturbations, for nG fields, are highly subdominant compared to those due to the inflationary scalar modes. More important in our context will be the Alfvén mode driven by the rotational component of the Lorentz force, especially since they decay without such magnetic driving. We recall below some features of their evolution (Jedamzik, Katalinic & Olinto 1998 (JKO); Subramanian & Barrow 1998 (SB98a)).

The Alfvén mode oscillates negligibly on Mpc Scales by recombination, with the phase of its oscillation $\chi = kV_A\eta \sim 10^{-2}B_{-9}(k/0.2h\mathrm{Mpc}^{-1})(\eta/\eta_*)$. Here the Alfvén velocity is $V_A \sim 3.8\times 10^{-4}cB_{-9}$, k the comoving wavenumber, η the conformal time with η_* its value at recombination. Unlike the compressional mode, which gets strongly damped below the Silk scale L_S due to radiative viscosity (Silk 1967), the Alfvén mode behaves like an over-damped oscillator. Note that for an over-damped oscillator there is one normal mode which is strongly damped and another one where the velocity starts from zero and freezes at the terminal velocity till the damping becomes weak at a latter epoch. The net result is that the Alfvén mode survives Silk damping for scales bigger than $L_A \sim (V_A/c)L_S \ll L_S$, the canonical Silk damping scale (JKO; SB98a). The resulting baryon velocity is potentially detectable, since due to the Doppler effect, CMB temperature anisotropies $\Delta T/T \sim V/c \sim f_d\chi V_A/c \sim 10^{-3}f_d\chi(B_{-9}/3)$ are induced. Here $f_d < 1$ takes into account possible damping effects due the thickness of the last scattering surface. One sees that for nG fields, significant temperature anisotropies with $\Delta T/T \sim 10^{-6}$ can result, even for $f_d\chi \sim 10^{-3}$. Detailed computations bear out this simple estimate and show that the signal peaks on arc minute scales, $l \sim 10^3$ (corresponding to the angle subtended by the Silk scale at recombination), and because $L_A \ll L_{Silk}$, it is significant even below the Silk scale.

After recombination, when radiation decouples from the baryons, the cosmic pressure drops by a large factor of order the photon to baryon ratio, $n_\gamma/n_b \gg 1$. The surviving tangled magnetic fields can now drive strong compressible motions and seed density fluctuations (Wassermann 1978; SB98a; Sethi 2003), which could well be very important in forming the first structures and leading to an early reionization of the Universe (Sethi & Subramanian 2005).

3. CMB signals from tangled magnetic fields

CMB anisotropies in general arise in two ways. Firstly, spatial inhomogeneities around the surface of last scattering of the CMB lead to the 'primary' anisotropies in the CMB temperature as seen at present epoch. Furthermore, variations in intervening gravitational and scattering effects, which influence the CMB photons as they come to us from the last scattering surface, can lead to additional secondary anisotropies (cf. Subramanian 2005 for a review). The CMB temperature anisotropies $\Delta T(\theta,\phi)/T$ are expanded in spherical harmonics,

$$\frac{\Delta T}{T}(\theta,\phi) = \sum_{lm} a_{lm}Y_{lm}(\theta,\phi); \quad a_{lm}^* = (-1)^m a_{l-m}, \quad (1)$$

and expressed in terms of their angular power spectrum C_l where the ensemble average $\langle a_{lm}a_{l'm'}^*\rangle = C_l\delta_{ll'}\delta_{mm'}$. The mean square temperature fractional anisotropy is given by

$$\frac{\langle(\Delta T)^2\rangle}{T^2} = \sum_l C_l\frac{2l+1}{4\pi} \approx \int \frac{l(l+1)C_l}{2\pi}\, d\ln l$$

with the last approximate equality valid for large l. So $(l(l+1)C_l)/2\pi$ measures the power in the temperature anisotropies per logarithmic interval in l space. (This combination is used because scale-invariant potential perturbations generate anisotropies, which at large scales (small l) have a nearly constant $l(l+1)C_l$). A convenient characterization of the scale-dependent temperature anisotropy is $\Delta T(l) = T[l(l+1)C_l)/2\pi]^{1/2}$. This is plotted in Figure 1, as a dashed-triple-dotted line for a standard ΛCDM model.

Primordial magnetic fields induce a variety of additional signals on the CMB. An uniform field would for example select out a special direction, lead to anisotropic expansion around this direction, hence leading to a quadrupole anisotropy. The degree of isotropy of the CMB then implies a limit of several nG on such a field (Barrow, Ferreira & Silk 1997). Comparable limits may obtain, at least for the uniform component, from upper limits to the IGM Faraday rotation of high redshift quasars (cf. Blasi et al. 1999). For inhomogeneous, tangled primordial fields, the spatial inhomogeneities around the surface of last scattering, due to magnetically induced perturbations (scalar, vector and tensor), lead to both large and small angular scale anisotropies in the CMB temperature and polarization.

For magnetically induced scalar perturbations, the question of the initial conditions has only been analyzed in some detail recently in a paper by Giovannini (2004), and detailed predictions of the CMB anisotropies, for general initial conditions, are yet to be worked out. (For some approximate treatments of the magnetosonic scalar modes see Adams et al. 1996; Koh & Lee 2000; Yamazaki, Ichiki & Kajino 2005). Further, scalar modes are dominated by the standard inflationary scalar perturbation and are also damped by radiative viscosity below the Silk scale.

Much more work has been done on the vector modes (Subramanian & Barrow 1998 (SB98b), 2002 (SB02); Seshadri & Subramanian 2001 (SS01); Mack, Kahniashvilli & Kosowsky 2002; Subramanian, Seshadri & Barrow 2003 (SSB03); Lewis 2004). They typically lead to a temperature anisotropy $\Delta T \sim 5\mu\mathrm{K}\,(B_{-9}/3)^2$ at $l \sim 1000$ and above (see below). A comparable signal arises at large angular scales, $l < 100$, due to gravitational wave perturbations (tensors). All modes lead to much smaller polarization signals. The

tensor and vector components in particular also lead to B-type polarization, which can help distinguish magnetic field induced signals from those due to inflationary scalar modes.

In addition, the presence of tangled magnetic fields in the intergalactic medium can cause Faraday rotation of the polarized component of the CMB, leading to the generation of new B-type signals from the inflationary E-mode signal. Their damping in the pre-recombination era can lead to spectral distortions of the CMB (Jedamzik, Katalinic & Olinto 2000), while their damping in the post-recombination era can change the ionization and thermal history of the Universe. A potentially important consequence which we discuss below is the magnetic field induced structure formation, which may be relevant to explain the early re-ionization implied by the WMAP data. We discuss some of these effects further below, focusing in more detail on vector modes and post recombination effects, where we have been directly involved in the computation of the magnetic signals.

3.1. Vector modes

On galactic scales and above, the induced velocity due to the Lorentz forces is generally so small that it does not lead to any appreciable distortion of the initial field (JKO; SB98a). Hence, the magnetic field simply redshifts away as $\mathbf{B}(\mathbf{x},t) = \mathbf{b}_0(\mathbf{x})/a^2$. The Lorentz force associated with the tangled field $\mathbf{F}_L = \mathbf{F}/(4\pi a^5)$, with $\mathbf{F} = (\nabla \times \mathbf{b}_0) \times \mathbf{b}_0$, pushes the fluid to create rotational velocity perturbations. These can be estimated by using the Navier-Stokes equation for the baryon-photon fluid in the expanding Universe,

$$\left(\frac{4}{3}\rho_\gamma + \rho_b\right)\frac{\partial v_i}{\partial t} + \left[\frac{\rho_b}{a}\frac{da}{dt} + \frac{k^2\eta}{a^2}\right]v_i = \frac{P_{ij}\hat{F}_j}{4\pi a^5}. \qquad (2)$$

Here, ρ_γ is the photon density, ρ_b the baryon density, and $\eta = (4/15)\rho_\gamma l_\gamma$ the shear viscosity coefficient associated with the damping due to photons, where l_γ is the photon mean free path. The projection tensor, $P_{ij}(\mathbf{k}) = [\delta_{ij} - k_i k_j/k^2]$ projects $\hat{\mathbf{F}}$, the Fourier component of $\mathbf{F}$ onto its transverse components perpendicular to $\mathbf{k}$.

One can solve Eq. 2 in two asymptotic limits, which allows semi-analytic estimates of the signals. For scales larger than the Silk scale, $kL_S < 1$, the radiative viscous damping can be neglected to get $v_i = 3P_{ij}\hat{F}_j D(\eta)/(16\pi\rho_0)$, where $D(\eta) = \eta/(1+R_*)$. Since $|\hat{F}_{ij}| \sim kV_A^2$, we get for large scales $v/c \sim \chi V_A/c$, as in our earlier simple estimate. For scales smaller than the Silk scale, $kL_S > 1$, one assumes a terminal velocity approximation to balance viscous damping with the driving due to the Lorentz force. This then leads to $D(\eta) \sim 5/ck^2L_\gamma$, and $v/c \sim (5/kL_\gamma)V_A^2/c^2$, where L_γ is the co-moving photon mean free path.

The angular power spectrum C_l of CMB anisotropies due to rotational velocity perturbations is given by (Hu & White 1997 (HW97))

$$C_l = 4\pi\int_0^\infty \frac{k^2dk}{2\pi^2}\quad\frac{l(l+1)}{2} \times \quad <|\int_0^{\eta_0} d\eta g(\eta_0,\eta)v(k,\eta)\frac{j_l(k(\eta_0-\eta))}{k(\eta_0-\eta)}|^2> \qquad (3)$$

Here $v(k,\eta)$ is the magnitude of the rotational component of the fluid velocity v_i in Fourier space, and η_0 the present value of η. The 'visibility function' $g(\eta_0,\eta)$ determines the probability that a photon reaches us at epoch η_0 if it was last scattered at the epoch η. So it weighs the contribution at any conformal time η by the probability of last scattering from that epoch. We have shown as a solid line in Fig. 3 the visibility function for a standard ΛCDM model. The spherical Bessel function of order l, the $j_l(z)$ term, projects variations in space, at the conformal time η around the last scattering epoch, to angular (or l) anisotropies at the present epoch. These spherical Bessel functions generally peak around $k(\eta_0-\eta) \approx l$. The multipoles l are then probing generally spatial scales with wavenumber $k \sim l/(\eta_0-\eta)$ at around last scattering.

We assume that $\mathbf{b}_0$ is a Gaussian random field. Its Fourier components satisfy $< b_i(\mathbf{k})b_j^*(\mathbf{q}) >= \delta_{\mathbf{k},\mathbf{q}}P_{ij}(\mathbf{k})M(k)$, where the magnetic power spectrum is normalized using a top hat filter in k-space, and taking $k^3M(k)/(2\pi^2) = (B_0^2/2)(n+3)(k/k_G)^{3+n}$ with $n > -3$. We generally normalize the field at $k_G = 1$ h Mpc^{-1}. The spectrum is cut-off at k_c, determined by dissipative processes.

An analytic estimate of the temperature anisotropy, for $kL_S < 1$ is then (SB98b; SB02)

$$\Delta T_B(l) \approx 5.8\mu K\left(\frac{B_{-9}}{3}\right)^2\left(\frac{l}{500}\right)I(\frac{l}{R_*}), \qquad (4)$$

whereas for scales smaller than Silk scales with $kL_S > 1$,

$$\Delta T_B(l) \approx 13.0\mu K\left(\frac{B_{-9}}{3}\right)^2\left(\frac{l}{2000}\right)^{-3/2}I(\frac{l}{R_*}). \qquad (5)$$

Here $I(k)$ is a mode coupling integral

$$I^2(k) = \frac{8}{3}(n+3)(\frac{k}{k_G})^{6+2n}; \quad n < -3/2$$
$$= \frac{28}{15}\frac{(n+3)^2}{(3+2n)}(\frac{k}{k_G})^3(\frac{k_c}{k_G})^{3+2n}; \quad n > -3/2.$$

Note that for $n < -3/2$, I is independent of k_c. For a nearly scale-invariant spectrum, say with $n = -2.9$, we get $\Delta T(l) \sim 4.7\mu\mathrm{K}\,(l/1000)^{1.1}$ for scales larger than the Silk scale, and $\Delta T(l) \sim 5.6\mu\mathrm{K}\,(l/2000)^{-1.4}$ for scales smaller than L_S but larger than L_γ. Larger signals will be expected for steeper spectra, $n > -2.9$ at the higher l end.

One can also do a similar calculation for the expected CMB polarization anisotropy (SS01; SSB03). Note that polarization of the CMB arises due to Thomson scattering of radiation from free electrons and is sourced by the quadrupole component of the CMB anisotropy. For vector perturbations, the B-type contribution dominates the polarization anisotropy (HW97), unlike for inflationary scalar modes. Further, as mentioned earlier, the vector mode signals can also be important below the Silk damping scale ($l \geq 10^3$).

We show in Figs. 1 and 2 the temperature and polarization anisotropy for the magnetic field induced vector modes obtained by evaluating the η and k integrals in Eq. (3) numerically. We retain the analytic approximations to $I(k)$ and $v_i(k)$. These curves show the build up of power in temperature and B-type polarization due to vortical perturbations from tangled magnetic fields which survive Silk damping at

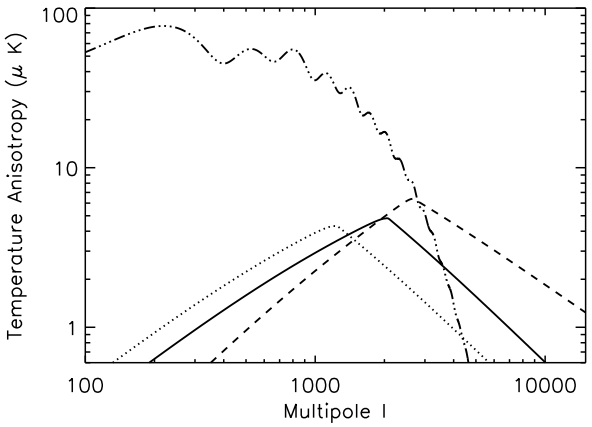

Fig. 1. ΔT versus l predictions for different cosmological models and $M(k) \propto k^n$, for $B_{-9} = 3$. The bold solid line is for a canonical flat, Λ-dominated model, with $\Omega_\Lambda = 0.7$, $\Omega_m = 0.3$, $\Omega_b h^2 = 0.02$, $h = 0.7$ and almost scale-invariant spectrum $n = -2.9$. The dotted curve (....) obtains when one changes to $\Omega_m = 1$ and $\Omega_\Lambda = 0$ model. The dashed line is for the Λ-dominated model with a larger baryon density $\Omega_b h^2 = 0.03$, and a larger $n = -2.5$. We also show for qualitative comparison (dashed-triple dotted curve), the temperature anisotropy in a 'standard' ΛCDM model, computed using CMBFAST (Seljak & Zaldarriaga 1996) with cosmological parameters as for the first model described above. (Adapted from SB02 and SSB03)

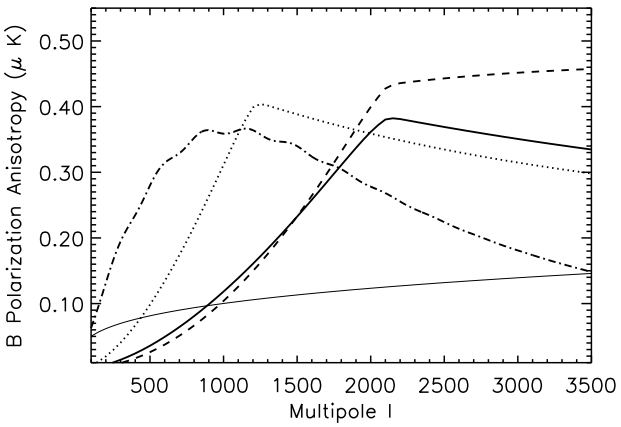

Fig. 2. ΔT_P^{BB} versus l predictions for different cosmological models and magnetic power spectrum $M(k) \propto k^n$, for $B_{-9} = 3$. The bold solid line is for a standard flat, Λ-dominated model, with $\Omega_\Lambda = 0.73$, $\Omega_m = 0.27$, $\Omega_b h^2 = 0.0224$, $h = 0.71$ and almost scale invariant spectrum $n = -2.9$. The dashed curve obtains when one changes to $n = -2.5$. The dotted curve gives results for a $\Omega_m = 1$ and $\Omega_\Lambda = 0$ model, with $n = -2.9$. We also show for qualitative comparison (dashed-dotted curve), the B-type polarization anisotropy due to gravitational lensing, in the canonical ΛCDM model, computed using CMBFAST (Seljak & Zaldarriaga 1996). The signal due to magnetic tangles dominate for l larger than about 1000. Finally, the thin solid line gives the expected galactic foreground contribution estimated by Prunet et al. (1998), which is also smaller than the predicted signals. (Adapted from SSB03)

high $l \sim 1000 - 3000$. The eventual slow decline is due to the damping by photon viscosity, which is only a mild decline as the magnetically sourced vortical mode is over damped. By contrast, in the absence of magnetic tangles there is a sharp cut-off due to Silk damping. Our numerical results are consistent analytic estimates given in Eqs. (4) and (5). A scale-invariant spectrum of tangled fields with $B_0 = 3 \times 10^{-9}$ Gauss, produces reduces temperature anisotropies at the 5μK level and B-type polarization anisotropies $\Delta T_B \sim 0.3 - 0.4\mu$K between $l \sim 1000 - 3000$. Larger signals result for steeper spectra with $n > -3$. Note that the anisotropies in hot or cold spots could be several times larger, because the non-linear dependence of C_l on $M(k)$ will imply non-Gaussian statistics for the anisotropies.

These magnetically induced signals could therefore contribute to the excess power detected by the CBI experiment. A distinguishing feature, compared to say the Sunyaev-Zeldovich (SZ) effect (Zeldovich & Sunyaev 1969) canonically invoked to explain the CBI excess, will be provided by the B-type polarization signals. Note that if the observed excess power in the CBI experiment arises from the SZ effect, this is not expected to be strongly polarized. The spectral dependence of the SZ signal could also help to distinguish it from any magnetically induced signals, which are expected to be frequency independent, at least at high frequencies.

Recently, Lewis (2004) has done a detailed numerical computation of the vector mode signal and finds qualitatively similar results to the semi-analytical estimates given above.

3.2. Tensor modes

Tangled magnetic fields also produce anisotropies on large angular scales, or small l, dominated by tensor metric perturbations induced by anisotropic magnetic stresses (Durrer, Ferreira & Kahniashvili 2000; Mack, Kahniashvili & Kosowsky 2002; Caprini & Durrer 2002; Giovannini 2005b). The tensor metric perturbation h_{ij} obeys the equation

$$h''_{ij} + 2\mathcal{H}h'_{ij} - \nabla^2 h_{ij} = -16\pi G a^2 \delta T^{TT}_{ij}$$

where $\mathcal{H} = a'/a$, a prime denotes derivative with respect to the conformal time, and δT^{TT}_{ij} is the transverse, traceless component of the energy momentum tensor (due to the magnetic field). The resulting CMB anisotropy is then computed using

$$(\Delta T/T) = -\frac{1}{2}\int_{\eta_i}^{\eta_0} h'_{ij} n^i n^j d\eta$$

where n^i is a unit vector along the line of sight, and prime denotes a conformal time derivative. Using the formalism described in these papers, we estimate a tensor contribution at small $l < 100$ of $\Delta T \sim 7(B_{-9}/3)^2 (l/100)^{0.1}\mu$K, for $n = -2.9$. (One has to account for neutrino anisotropic stress compensation (Lewis 2004) after neutrino decoupling). Since we have to add this power to the standard power produced by inflationary scalar perturbations in quadrature, a

tangled field with $B_{-9} \sim 3$ will produce of order a few to 10 percent perturbation to the power in the standard CMB anisotropy at large angular scales. So if they are indeed detected at large l, below the Silk damping scale, one will also have to consider their effects seriously at large angular scales, especially in cosmological parameter estimation. The tensor mode also contributes to the B-type polarization anisotropy at large angular scales ($l < 100$ or so), with $\Delta T_B < 0.1\mu$K for $B_{-9} < 3$. The production of gravitational waves has been used in an indirect manner by Caprini & Durrer (2002) to set strong upper limits on B_0 for spectra with $n > -2.5$ or so.

3.3. Faraday rotation due to primordial fields

Another interesting effect of primordial fields is the the Faraday rotation it induces on the polarization of the CMB (Kosowsky & Loeb 1996; Kosowsky et al. 2005; Campanelli et al. 2005). The rotation angle is about

$$\Delta\Phi \;=\; \lambda_0^2\,(3/e)\int_0^{\eta_0} d\eta' g(\eta_0,\eta')\mathbf{n}\cdot\mathbf{B}_0[\mathbf{n}(\eta'-\eta_0)]$$
$$\approx\; 1.6^o B_{-9}(\nu/30\mathrm{GHz})^{-2}$$

where λ_0 is the wavelength of observation. So this effect is important only at low frequencies, and here it can lead to the generation of B-mode polarization from the Faraday rotation of the inflationary E-mode. From the work of Kosowsky et al. (2005) one can estimate a B-mode signal $\Delta T_B \sim 0.4(B_{-9}/3)\,(\nu/30\mathrm{GHz})^{-2}\mu$K, for $n = -2$, at $l \sim 10^4$. The signals are smaller at smaller n. The Faraday rotation signal can be distinguished from the B-mode polarization generated by say vector modes, or gravitational lensing, because of their frequency dependence (ν^{-2}).

4. Post recombination blues

After recombination the Universe became mostly neutral, resulting also in a sharp drop in the radiative viscosity. Primordial magnetic fields can then dissipate their energy into the intergalactic medium (IGM) via ambipolar diffusion and, for small enough scales, by generating decaying MHD turbulence. These processes can significantly modify the thermal and ionization history of the post-recombination Universe. We show in Fig. 3 the modified visibility function due to the gradual re-ionization by ambipolar damping and turbulence decay from the work of Sethi & Subramanian (2005).

These dissipative processes, for $B_{-9} \sim 3$, can give rise to Thomson scattering optical depths $\tau \gtrsim 0.1$, although not in the range of redshifts needed to explain the recent WMAP polarization observations (the T-E cross correlation seen at low l). However, future CMB probes like PLANCK can potentially detect the modified CMB anisotropy signal from such partial re-ionization (Kaplinghat et al. 2003). This can be used to detect or further constrain small-scale primordial fields.

Potentially more exciting is the possibility that primordial fields could induce the formation of subgalactic structures for $z \gtrsim 15$. We show in Fig. 4 the mass dispersion $\sigma(R,z)$ for two models with nearly scale-free magnetic field

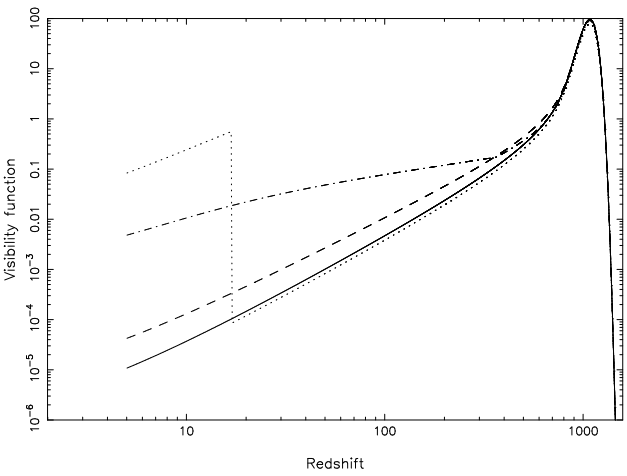

Fig. 3. Visibility function for different models. The solid and the dotted curves are for the standard recombination and a model in which the Universe re-ionizes at $z = 17$, respectively. The dashed curve corresponds to a decaying turbulence model with $B_0 = 3 \times 10^{-9}$ G. The dot-dashed curve corresponds to the ambipolar diffusion case with $B_0 = 3 \times 10^{-9}$ G and $n = -2.8$. (Adapted from SS05)

power spectra, as computed by SS05. When R is normalized to the magnetic Jeans scale, λ_J, it turns out that σ depends only on the ratio R/λ_J and not explicitly on the strength of the field. This interesting feature arises because density fluctuations are generated by the divergence of $\mathbf{F}_L$ and so are $\propto k^2 B_0^2$. Since the magnetic Jeans scale $\lambda_J \propto k_J^{-1} \propto B_0$, the magnetic field dependence cancels out in σ when scales are expressed in terms of R/λ_J (see SS05 for details). Structures collapse when $\sigma > 1$ (for the the spherical top hat model when $\sigma = 1.68$). For the nearly scale-free power law models, even typical structures at the magnetic Jeans scale collapse at high redshifts in the range between 10 to 20.

The mass of these objects does depend on the magnetic field strength smoothed to the Jeans scale, and lie in the range $10^9 M_\odot$ to $3 \times 10^{10} M_\odot$ for $B_0 \sim 10^{-9}$ G to $B_0 \sim 3 \times 10^{-9}$ G. An even smaller field could have a major impact, provided the collapsing structures have a mass larger than the thermal Jeans mass. For example, a field as small as $B = 0.1$ nG can induce a $10^6 M_\odot$ dwarf galaxy collapse at high z ($z > 15$), causing early enough re-ionization to explain the T-E cross correlation peak observed by WMAP. More detailed work on this aspect is underway.

5. Conclusions

We briefly reviewed some of the possible ways one could detect/constrain primordial magnetic fields using the CMB anisotropies and polarization. This endeavor would be even more fruitful if there were a compelling mechanism for primordial magnetognesis, which also produced strong enough ($B_{-9} \sim 1$) and coherent enough (ordered on Mpc scales) fields. At this juncture, theoretical predictions are highly parameter dependent, and so we have taken a more pragmatic approach of assuming that such a field could be generated in

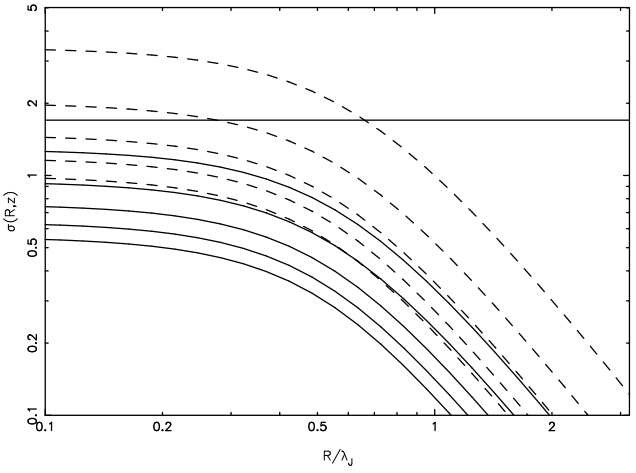

Fig. 4. The mass dispersion $\sigma(R, z)$ is shown for two models with nearly scale free magnetic field power spectra. The solid and dashed curves correspond to $n = -2.9$ and $n = -2.8$, respectively. Different curves, from top to bottom, correspond to redshifts $z = \{10, 15, 20, 25, 30\}$, respectively. The horizontal line corresponds to $\sigma = 1.68$. (Adapted from SS05)

the early Universe and asking what it would imply for the CMB and structure formation in general.

For a field of $B \sim 3$ nG and a nearly scale-invariant spectrum one predicts CMB temperature anisotropies with a $\Delta T \sim 5\mu$K, at $l < 100$ and $l > 1000$ and polarization anisotropies with $\Delta T_P \sim 0.4\mu$K at $l > 1000$. Especially interesting is that the vector modes induced by primordial fields can contribute significantly below the Silk scale, where the conventional scalar modes are exponentially damped. Further, the magnetically induced signal at small angular scales will be dominated by B-mode polarization. There do exist intriguing results from the CBI experiment for the presence of a temperature excess at small angular scales. Some part of this excess could arise due to the influence of primordial fields. This excess is conventionally explained as arising due to the SZ effect, but the power in density fluctuations on cluster scales (conventionally measured by σ_8), has to be pushed to be in the upper range of values ($\sigma_8 \sim 1$), allowed by current CMB and large-scale structure data. Since the SZ signal is frequency dependent, a crucial test would be to compare CMB observations at different frequencies.

Also if B-type polarization at these scales is detected this could be a good indicator of the magnetic field effects. Clearly it will be important to make further observations at small angular scales, especially at different frequencies. It is also important to study the statistics of the CMB anisotropies, since the magnetically induced signals are predicted to be strongly non-Gaussian. If magnetic fields have helicity, this would induce further interesting effects, which have been reviewed in this meeting (Kahniashvilli 2006 and references therein).

We have also emphasized another interesting consequence of the existence of primordial magnetic fields, which indirectly affects the CMB anisotropies. Due to their presence the first collapsed objects of dwarf galaxy masses and smaller can form at high $z > 15$, even for $B \sim 0.1$ nG. This can potentially lead to the early re-ionization indicated by the present WMAP polarization data in a very natural manner.

Acknowledgements. Much of the work reviewed here are in joint papers with John Barrow, T. R. Seshadri and Shiv Sethi. I thank them for very enjoyable collaborations, Dmitri Sokoloff for useful comments, and the SKA Project Office for partial support.

References

Adams, J., Danielsson, U., Grasso, D. Rubinstein, H.: 1996, Physics Letters B 388, 253
Barrow, J.D., Ferreira, P.G., Silk, J.: 1997, PRL 78, 3610
Blasi, P., Burles, S., Olinto, A.: 1999, ApJ 514, L79
Brandenburg, A., Subramanian, K.: 2005, Phys. Rep. 417, 1
Campanelli, L., Dolgov, A., Giannotti, M., Villante, F.: 2005, ApJ 616, 1
Caprini, C., Durrer, R.: 2002, PRD 65, 23517
Durrer, R., Ferreira, P.G., Kahniashvili, T.: 2000, PRD 61, 043001
Gasperini, M.: 2006, AN, this volume (astro-ph/0509174)
Giovannini, M.: 2004, PRD 70, 123507
Giovannini, M.: 2005a, Int. J. Mod. Phys. D13, 391
Giovannini, M.: 2005b, astro-ph/0508544
Grasso, D., Rubinstein, H.R.: 2001, Phys. Rep. 348, 161
Hu, W., White, M.: 1997, PRD 56, 596
Jedamzik, K., Katalinić, V., Olinto, A.V.: 1998, PRD 57, 3264
Jedamzik, K., Katalinić, V., Olinto, A.V.: 2000, PRL 85, 700
Kahniashvilli, T.: 2006, AN, this volume (astro-ph/0510151).
Kaplinghat, M., Chu, M., Haiman, Z., Holder, G.P., Knox, L., Skordis, C.: 2003, ApJ 583, 24
Kosowsky, A., Loeb, A.: 1996, ApJ 469, 1
Kosowsky, A, Kahniashvili, T., Lavrelashvili, G., Ratra, B.: 2005, PRD 71, 043006
Lewis, A.: 2004, PRD 70, 043011
Mack, A., Kashniashvili, T., Kosowsky, A.: 2002, PRD 65, 123004
Prunet, S., Sethi, S.K., Bouchet, F.R., Miville-Deschenes, M.A.: 1998, A&A 339, 187
Ratra, B.: 1992, ApJ 391, L1
Readhead, A.C.S., et al.: 2004, ApJ 609, 498
Schekochihin, A., Cowley, S., Kulsrud, R., Hammett, G., Sharma, P.: 2005, ApJ 629, 139
Seljak, U., Zaldarriaga, M.: 1996, ApJ 469, 437
Silk, J.: 1968, ApJ 151, 431
Seshadri, T.R., Subramanian, K.: 2001, PRL 87, 101301
Sethi, S.K.: 2003, MNRAS 342, 962
Sethi, S.K., Subramanian, K.: 2005, MNRAS 356, 778
Shukurov, A., Subramanian, K., Haugen, N.E.L.: 2006, AN, this volume (astro-ph/0512608).
Spergel, D. N., et al.: 2003, ApJS 148, 175
Subramanian, K.: 2005, Current Science 88, 1068
Subramanian, K., Barrow, J.D.: 1998, PRD 58, 83502
Subramanian, K., Barrow, J.D.: 1998, PRL 81, 3575
Subramanian, K., Barrow, J.D.: 2002, MNRAS 335, L57
Subramanian, K., Seshadri, T.R., Barrow, J.D.: 2003, MNRAS 344, L31
Subramanian, K., Shukurov, A., Haugen, N.E.L.: 2006, MNRAS (in press) (astro-ph/0505144)
de Oliveira-Costa, A., Tegmark, M., Zaldarriaga, M., Hamilton, A.: 2004, PRD 69, 063516
Turner, M.S., Widrow, L.M.: 1988, PRD 37, 2743
Wasserman, I.: 1978, ApJ 224, 337
Widrow, L.M.: 2002, Rev. Mod. Phys. 74, 775
Yamazaki, D.G., Ichiki, K., Kajino, T.: 2005, ApJ 625, L1
Zeldovich, Y.B., Sunyaev, R.A.: 1969, Ap&SS 4, 301